

# Sequential adaptive design for emulating costly computer codes

Hossein Mohammadi\* and Peter Challenor

College of Engineering, Mathematics and Physical Sciences, University of Exeter,  
Exeter, UK

## Abstract

Gaussian processes (GPs) are generally regarded as the gold standard surrogate model for emulating computationally expensive computer-based simulators. However, the problem of training GPs as accurately as possible with a minimum number of model evaluations remains a challenging task. We address this problem by suggesting a novel adaptive sampling criterion called VIGF (variance of improvement for global fit). It is the variance of an improvement function which is defined at any location as the square of the difference between the fitted GP emulator and the model output at the nearest site in the current design. At each iteration of the proposed algorithm, a new run is performed where the VIGF criterion is the largest. Then, the new sample is added to the design and the emulator is updated accordingly. The batch version of VIGF is also proposed which can save the user time when parallel computing is available. The applicability of our method is assessed on a number of test functions and its performance is compared with several sequential sampling strategies. The results suggest that our method has a superior performance in predicting the benchmarking functions in most cases.

**Keywords:** Computer experiments; Gaussian processes; Numerical simulation; Sampling strategies

## 1 Introduction

This paper deals with adaptive design of experiment (DoE) for Gaussian process (GP) models [46] in the context of emulating complex computer codes. This problem is of great importance to many applications where time-consuming simulators are employed to study a physical system; see e.g., [28, 36, 42]. Due to computational burden of such models, we only

---

\*Corresponding Author: h.mohammadi@exeter.ac.uk

have access to a limited number of simulation runs. As a result, conducting analysis such as uncertainty/sensitivity analysis [49] that requires a huge number of model evaluations becomes impossible. One way around this computational complexity is to approximate the model by a cheap-to-evaluate surrogate model. A review of the most common surrogates can be found in [1, 16]. Among them, GP emulators have become a standard in the field of computer experiments due to their flexibility and inherent estimation of prediction uncertainty [48, 50].

GPs are constructed based on a set of (carefully-designed) training runs called *design points*. The locations of those points have a consequential effect on the predictive performance of GPs. It is a challenging task to build an emulator as accurately as possible with a minimum number of calls to the computationally intensive simulator. This problem is an active area of research with important applications [3, 38, 8]. It is tackled via different approaches which can be divided into two groups:

- (I) *One-shot DoE* where all the design locations are chosen at once, in advance of building the emulator. In this framework, all regions of the input space are treated as equally important, and points are spread across the space as uniformly as possible. Such *space-filling* design can be generated using e.g., maximin or minimax [25] criterion. A maximin-based design, for example, is attained by maximising the minimal distance between all candidate points. Latin hypercube sampling (LHS) [40], full factorial [6], orthogonal array [44], and uniform designs [11] are examples of the one-shot DoE. Since the number of design points is decided beforehand in such DoE, there is the risk of under/oversampling [53, 15] which is a critical issue in sampling from computationally expensive simulators. A space-filling design can also be achieved using sequential sampling approaches such as Halton [19] or Sobol [55] sequences. These methods, however, do not consider output information and differ from adaptive strategies explained below.
- (II) *Adaptive DoE* in which the choice of the next input value depends on the previously observed responses. Generally, the implementation of adaptive sampling algorithms is more cumbersome than one-shot ones. However, adaptive methods do not suffer from under/oversampling as we can stop them once the emulator reaches an adequate level of accuracy. This is a desirable property when emulating costly computer codes. Also, an adaptive design allows us to sample more points in “interesting” regions, e.g., where the model response is highly nonlinear or changes rapidly. The focus of this paper is on the GP-based adaptive sampling. We refer the reader to recent papers [14, 34] for a comprehensive survey of the existing methods in this regard.

An adaptive sampling method generally needs to make a trade-off between two concepts: *exploitation* and *exploration*. The former aims to concentrate the search on identified interesting regions and sample more points there. The latter seeks poorly-represented parts of the domain to discover the interesting regions that have not yet been detected

[34, 15]. For example, in [2, 23, 32, 35] the leave-one-out (LOO) cross-validation error accounts for exploitation, and a distance-based metric (often as a constraint optimisation) for exploration. The LOO error is obtained by removing a point from the training set, fitting a GP to the remaining data, and computing the difference between the actual response and its prediction. The magnitude of the LOO error at a design point is a measure of the sensitivity of the emulator to that point. In other words, the larger the LOO error is, the more important the design point becomes. Thus, the new sample should be taken near the point with the largest LOO error. [27, 59] suggested the idea of partitioning the input space using the Voronoi tessellation [57], and choosing the next design location in the cell with the largest LOO metric. The expected squared LOO (ES-LOO) error is introduced in [41] to guide exploitation. The ES-LOO error is estimated at unobserved locations by a second GP model. Then, a modified version of *expected improvement* [26, 51] is used to prevent new samples from clustering around the existing design. The performance of the adaptive sampling algorithm based on the ES-LOO criterion is compared with our proposed method in Section 4.

Variance-based methods are a classic way of doing adaptive DoE. In this sampling strategy, the GP predictive variance is considered as the prediction error which is the difference between the predictive mean and ground truth. The most common variance-based selection criteria are the mean squared error (MSE) [24, 48] and integrated MSE (IMSE) [45, 48]. The former is a measure of the distance between points relying on the canonical metric of the GP covariance function [38]. Thus, a sequential sampling based on maximising MSE can lead to a space-filling design as shown in Section 4. We note that since the MSE criterion does not depend on the output function values (see Section 2), a sequential design based on MSE is actually non-adaptive. The IMSE criterion presents the average accuracy of the emulator [45], and the new location is selected where IMSE is minimum. The point obtained this way causes a maximum reduction in the overall (integrated) prediction uncertainty. A potential drawback of the variance-based methods is that they are likely to favour points on the boundaries of the domain where the prediction uncertainty is large. Such points may not be informative since models are not often precisely known on the boundaries, and measurement error can be significant there [17].

Entropy-based adaptive DoE is the last category of sampling strategies we review here. Entropy, first introduced by Shannon [52], can be used to quantify the uncertainty in the outcome of a random variable. Entropy is a concept in information theory, and a maximum entropy design maximises the information gained [54]. In the GP paradigm, such design can be achieved by maximising the determinant of the covariance matrix of the sample points, and is analogous to a *D-optimal* design [7]. The maximum entropy algorithm suits sequential sampling, and is equivalent to the maximum MSE approach if only one new location is selected at each iteration [24]. On a different note, entropy-based adaptive criteria have been employed in Bayesian optimisation [20, 21], and estimating contours of costly functions [8, 39]. An alternative to the entropy criterion is *mutual information* [30]; it measures the amount of information that one random process provides about another. In

MICE (Mutual Information for Computer Experiments) [3], mutual information is defined between the GP fitted to the training data, and the emulator constructed based on a set of candidate points. Here, the search is performed over a discrete space and a point from the candidate set that provides the highest mutual information is selected for the next evaluation. We use MICE as a competitor adaptive DoE in Section 4.

The adaptive sampling algorithm proposed in this paper is based on an improvement metric. At any location, the improvement is defined as the square of the difference between the fitted emulator and the model output at the nearest site. The method, called *variance of improvement for global fit (VIGF)*, uses the variance of improvement as the selection criterion. At each iteration, a new point is selected where VIGF is the largest, and the emulator is updated with the new data. Section 3 describes more details on the proposed approach. We first provide the basics of GPs in the next section.

## 2 Gaussian process emulators

Suppose that we want to emulate the output of a deterministic computer code govern by the function  $f : \mathcal{D} \mapsto \mathbb{R}$ , where the input space  $\mathcal{D}$  is a compact set in the  $d$ -dimensional Euclidean space  $\mathbb{R}^d$ . Typically,  $f$  is a black-box function and its analytical expression is not known. A GP is a collection of random variables, any finite number of which follow a Gaussian distribution [46]. Let  $(Z_0(\mathbf{x}))_{\mathbf{x} \in \mathcal{D}}$  represent a GP. It is fully specified by its mean and covariance function/kernel that needs to be positive semi-definite. In this work, the GP mean (without loss of generality) is assumed to be a constant:  $m_0 = \mathbb{E}[Z_0(\mathbf{x})]$ . The covariance function  $k_0 : \mathcal{D} \times \mathcal{D} \mapsto \mathbb{R}$  is given by

$$k_0(\mathbf{x}, \mathbf{x}') = \text{Cov}(Z_0(\mathbf{x}), Z_0(\mathbf{x}')) = \sigma^2 \text{Corr}(Z_0(\mathbf{x}), Z_0(\mathbf{x}')), \forall \mathbf{x}, \mathbf{x}' \in \mathcal{D}, \quad (1)$$

where  $\sigma^2$  is the process variance, and regulates the scale of the amplitude of  $Z_0(\mathbf{x})$ . Covariance functions play a key role in the GP modelling as most assumptions about the form of  $f$  are encoded through them. There exist many types of kernels; a list of them can be found in [46, 48].

Now suppose that the model is evaluated at design locations  $\mathbf{X}_n = (\mathbf{x}_1, \dots, \mathbf{x}_n)^\top$  with the corresponding outputs  $\mathbf{y}_n = (f(\mathbf{x}_1), \dots, f(\mathbf{x}_n))^\top$ . Together,  $\mathbf{X}_n$  and  $\mathbf{y}_n$  create the training set  $\mathcal{A} = \{\mathbf{X}_n, \mathbf{y}_n\}$ . The posterior/predictive distribution of  $Z_0(\mathbf{x})$  is denoted by  $Z_n(\mathbf{x}) = Z_0(\mathbf{x}) \mid \mathcal{A}$  and is computed according to Bayes' rule. The posterior GP  $Z_n(\mathbf{x})$  is characterised by [46]

$$m_n(\mathbf{x}) = \mathbb{E}[Z_n(\mathbf{x})] = m_0 + \mathbf{k}(\mathbf{x})^\top \mathbf{K}^{-1}(\mathbf{y}_n - m_0 \mathbf{1}), \quad (2)$$

$$k_n(\mathbf{x}, \mathbf{x}') = \text{Cov}(Z_n(\mathbf{x}), Z_n(\mathbf{x}')) = k_0(\mathbf{x}, \mathbf{x}') - \mathbf{k}(\mathbf{x})^\top \mathbf{K}^{-1} \mathbf{k}(\mathbf{x}'), \quad (3)$$

wherein  $\mathbf{k}(\mathbf{x}) = (k_0(\mathbf{x}, \mathbf{x}_1), \dots, k_0(\mathbf{x}, \mathbf{x}_n))^\top$ , and  $\mathbf{1}$  stands for a vector of ones, and  $\mathbf{K}$  is an  $n \times n$  covariance matrix whose entries are:  $\mathbf{K}_{ij} = k_0(\mathbf{x}_i, \mathbf{x}_j)$ , for  $1 \leq i, j \leq n$ . The

predictive variance is given by  $s_n^2(\mathbf{x}) = k_n(\mathbf{x}, \mathbf{x})$ , and is equivalent to the MSE criterion

$$MSE(\mathbf{x}) = \mathbb{E} \left[ (Z_n(\mathbf{x}) - m_n(\mathbf{x}))^2 \right] = s_n^2(\mathbf{x}). \quad (4)$$

It is worth mentioning that the predictive mean interpolates the observations at the experimental designs and the predictive variance is zero there. Also, we have  $Z_n(\mathbf{x}) \sim \mathcal{N}(m_n(\mathbf{x}), s_n^2(\mathbf{x}))$ ,  $\forall \mathbf{x} \in \mathcal{D}$ .

### 3 Proposed adaptive design criterion

In this section, we introduce our adaptive sampling algorithm which relies on the VIGF criterion. At each iteration, a new site is selected where VIGF reaches its maximum. Then, the model is evaluated there to get the corresponding response. This new data is added to the current training set and the emulator is updated accordingly. Algorithm 1 outlines the steps of the proposed method. The building block of VIGF is the *improvement* function

---

**Algorithm 1** Proposed adaptive sampling algorithm

---

Input: training set  $\mathcal{A} = \{\mathbf{X}_n, \mathbf{y}_n\}$ , and prior GP  $(Z_0(\mathbf{x}))_{\mathbf{x} \in \mathcal{D}}$

- 1: Compute the posterior GP  $Z_n(\mathbf{x}) = Z_0(\mathbf{x}) \mid \mathcal{A}$
  - 2: **while not** stop **do**
  - 3:   Compute  $\mathbf{x}_{n+1} = \underset{\mathbf{x} \in \mathcal{D}}{\operatorname{argmax}} VIGF(\mathbf{x})$
  - 4:   Evaluate  $f$  at  $\mathbf{x}_{n+1}$  to have  $f(\mathbf{x}_{n+1})$
  - 5:   Set  $\mathbf{X}_{n+1} = \mathbf{X}_n \cup \{\mathbf{x}_{n+1}\}$  and  $\mathbf{y}_{n+1} = \mathbf{y}_n \cup \{f(\mathbf{x}_{n+1})\}$
  - 6:   Update  $Z_n(\mathbf{x})$  with  $(\mathbf{x}_{n+1}, y_{n+1})$
  - 7:    $n \leftarrow n + 1$
  - 8: **end while**
- 

defined as [31]

$$\mathcal{I}(\mathbf{x}) = (Z_n(\mathbf{x}) - f(\mathbf{x}_i^*))^2, \quad (5)$$

with  $\mathbf{x}_i^*$  being the design point closest (in Euclidean distance) to  $\mathbf{x}$ . The variance of  $\mathcal{I}(\mathbf{x})$  can be calculated knowing that  $\mathcal{I}(\mathbf{x})/s_n^2(\mathbf{x})$  has a noncentral chi-square distribution characterised by [41]

$$\mathcal{I}(\mathbf{x})/s_n^2(\mathbf{x}) \sim \chi'^2 \left( \kappa = 1, \lambda = \left( \frac{m_n(\mathbf{x}) - f(\mathbf{x}_i^*)}{s_n(\mathbf{x})} \right)^2 \right). \quad (6)$$

Here,  $\kappa$  and  $\lambda$  are the degree of freedom, and noncentrality parameter, respectively. The variance of the above distribution is  $4\lambda + 2\kappa$ :

$$\mathbb{V}(\mathcal{I}(\mathbf{x})/s_n^2(\mathbf{x})) = 4 \left( \frac{m_n(\mathbf{x}) - f(\mathbf{x}_i^*)}{s_n(\mathbf{x})} \right)^2 + 2. \quad (7)$$

Now, if both sides of the above equation are multiplied by  $s_n^4(\mathbf{x})$ , we reach the VIGF expression

$$VIGF(\mathbf{x}) = \mathbb{V}(\mathcal{I}(\mathbf{x})) = 4s_n^2(\mathbf{x})(m_n(\mathbf{x}) - f(\mathbf{x}_i^*))^2 + 2s_n^4(\mathbf{x}). \quad (8)$$

The terms  $s_n^2(\mathbf{x})$  and  $(m_n(\mathbf{x}) - f(\mathbf{x}_i^*))^2$  account for exploration and exploitation, respectively. These are called the variance and squared *bias* (with respect to  $f(\mathbf{x}_i^*)$ ) in conventional statistics, respectively. The former reflects the uncertainty of the emulator about its prediction and grows away from the training data. The latter gets large when the predictive mean  $m_n(\mathbf{x})$  deviates from  $f(\mathbf{x}_i^*)$  and, hence, captures the local behaviour of  $f$ . Equation (8) benefits from the interaction between exploration and exploitation. Such interaction causes VIGF to increase in regions where both components are critical.

It is notable that Lam [31] proposed *expected improvement for global fit (EIGF)* where the expected value of  $\mathcal{I}(\mathbf{x})$  serves as the selection criterion

$$EIGF(\mathbf{x}) = \mathbb{E}[\mathcal{I}(\mathbf{x})] = (m_n(\mathbf{x}) - f(\mathbf{x}_i^*))^2 + s_n^2(\mathbf{x}). \quad (9)$$

However, it is found that EIGF tends towards local exploitation and is susceptible to get stuck in an optimum [3, 37, 41]. The reason is that  $(m_n(\mathbf{x}) - f(\mathbf{x}_i^*))^2$  can act as a measure of gradient and grows when  $f(\mathbf{x}_i^*)$  is nearby an optimum. In this situation, the exploitation term plays a critical role and EIGF favours points around the optimum. Since the relationship between exploration and exploitation components in EIGF (Equation (9)) is additive, it cannot easily escape the basin of attraction. This is not the case for VIGF (Equation 8) where there is a multiplicative relation between the two components. As an example, Figure 1 visualises the sampling behaviour of EIGF (left) and VIGF (right). The underlying function  $f$  is a sum of two Gaussian functions. The black dots are the initial design, and the red circles represent the adaptive samples generated by the two approaches. As can be seen, EIGF overexploits the area around the centre of spike at  $(1/3, 1/3)^\top$  and puts a lot of samples there. In VIGF, the balance between exploration and exploitation is more efficient and the search is more global than EIGF.

**Extension to batch mode** In a batch mode sampling, a set of inputs are chosen for evaluation at each iteration. This can save the user time when parallel computing is available. Here, we propose the batch version of the VIGF criterion, called *pseudo VIGF (PVIGF)*. It is obtained by multiplying VIGF by a repulsion/influence function, first introduced in [60] for batch Bayesian optimisation. The repulsion function (RF) is defined as

$$RF(\mathbf{x}; \mathbf{x}_u) = 1 - \text{Corr}(Z_n(\mathbf{x}), Z_n(\mathbf{x}_u)), \quad (10)$$

with  $\mathbf{x}_u$  being an updating point. The RF function is zero at  $\mathbf{x}_u$  and tends to one as  $\|\mathbf{x} - \mathbf{x}_u\| \rightarrow \infty$ . With the RF function one can add new design locations (as updating points) to the current DoE without evaluating the expensive function  $f$ . This is illustrated in Figure 2 where the left panel shows a GP fitted to five design points (black dots), and

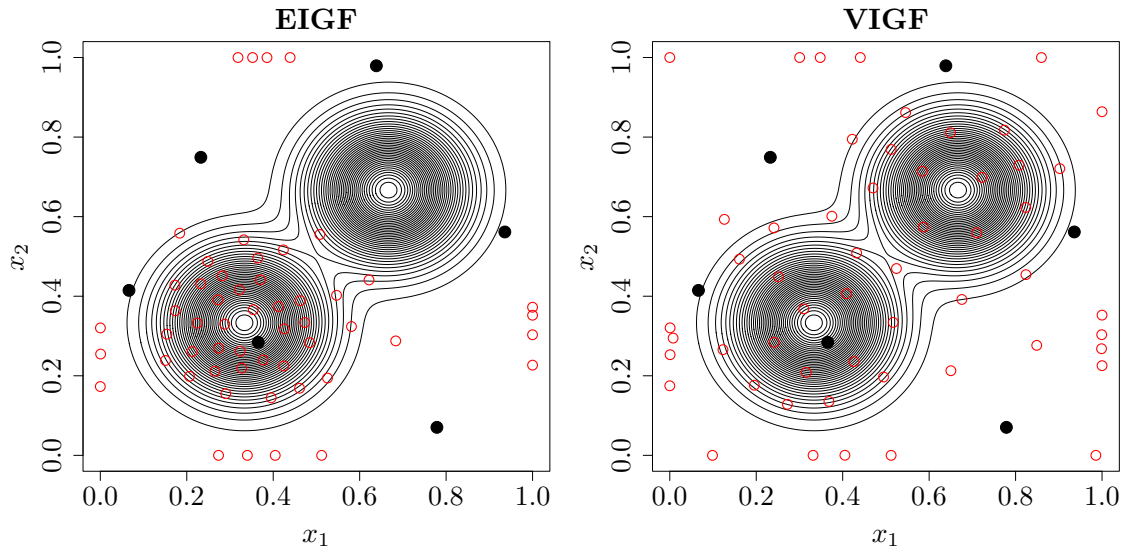


Figure 1: The sampling behaviour of EIGF (left) and VIGF (right) on a 2-dimensional problem which is a sum of two Gaussian functions. The black dots represent the initial design locations and red circles are the samples selected adaptively. EIGF takes many samples around the optimum  $(1/3, 1/3)^\top$ . VIGF has a more global search due to the interaction between exploration and exploitation components.

the corresponding VIGF criterion (right scale). In the right panel, the new location  $x_6$  (blue circle) at which VIGF is maximum is added to the existing design without evaluating  $f$  there. PVIGF (dashed red) is obtained by multiplying  $VIGF(x)$  by  $RF(x; x_6)$  (dash-dotted green). The pseudocode of the batch mode sampling is presented in Algorithm 2 where  $q > 1$  locations are added to  $\mathbf{X}_n$  at each iteration.

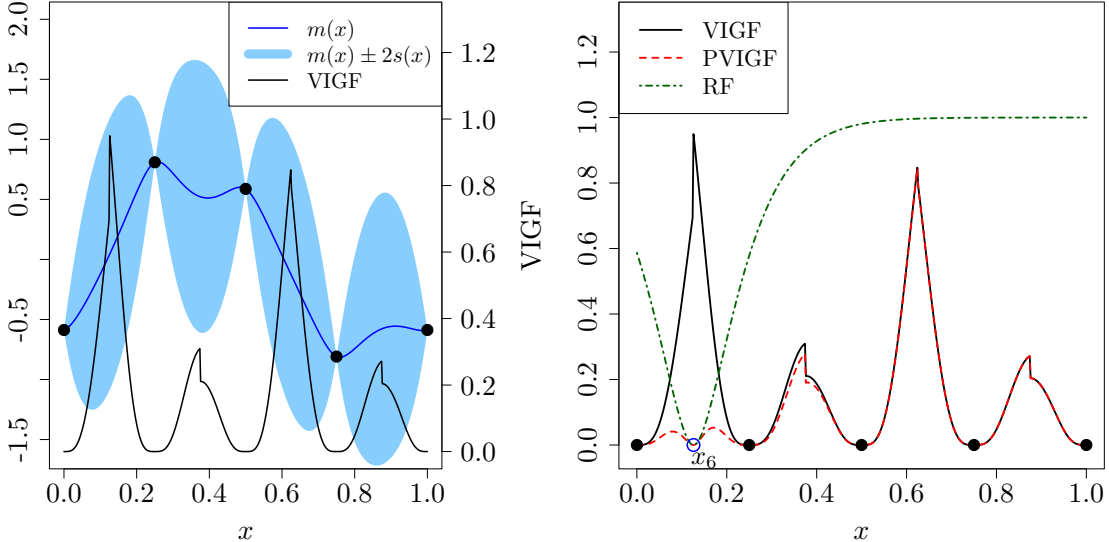


Figure 2: Left: A GP fitted to the five training data (black dots), and the corresponding VIGF function (right scale). Right: PVIGF (dashed red) is obtained by multiplying VIGF by the RF function (dash-dotted green) with the updating point  $x_6$  (blue circle).

## 4 Numerical experiments

The results of numerical experiments are provided in this section. The applicability of the proposed method is compared with several sampling schemes on a suite of frequently used analytical test functions as described below.

### 4.1 Test cases and experimental setup

Our proposed method is applied to eight benchmark problems which serve as the ground truth models. They are summarised in Table 1 and their analytical expression is given in Appendix A. The functions  $f_1 - f_6$  are defined on the hypercube  $[0, 1]^d$ . The problems  $f_7$  (OTL circuit) and  $f_8$  (piston simulation) are physical models. The former simulates the midpoint voltage of an OTL push-pull circuit and the latter computes the cycle time of a piston within a cylinder. The functions are classified into two groups according to



---

**Algorithm 2** Choosing a batch of  $q > 1$  locations at each iteration

---

Input: GP  $Z_n(\mathbf{x})$  which is constructed based on  $\mathcal{A} = \{\mathbf{X}_n, \mathbf{y}_n\}$ 

- 1: Create  $VIGF(\mathbf{x})$  using Equation (8)
- 2: Compute  $\mathbf{x}_{n+1} = \operatorname{argmax}_{\mathbf{x} \in \mathcal{D}} VIGF(\mathbf{x})$
- 3:  $PVIGF(\mathbf{x}) = RF(\mathbf{x}; \mathbf{x}_{n+1})VIGF(\mathbf{x})$
- 4: **for**  $j = 2$  to  $q$  **do**
- 5:   Compute  $\mathbf{x}_{n+j} = \operatorname{argmax}_{\mathbf{x} \in \mathcal{D}} PVIGF(\mathbf{x})$
- 6:    $PVIGF(\mathbf{x}) = RF(\mathbf{x}; \mathbf{x}_{n+j})PVIGF(\mathbf{x})$
- 7: **end for**

Output:  $\mathbf{x}_{n+1}, \mathbf{x}_{n+2}, \dots, \mathbf{x}_{n+q}$ 

---

their dimensionality: small-scale ( $1 \leq d \leq 4$ ) and medium-scale ( $5 \leq d \leq 8$ ) [29]. In order to assess the accuracy of the emulator, we use the *normalised root mean squared error* (NRMSE) criterion

$$NRMSE = \frac{\sqrt{\frac{1}{n_t} \sum_{t=1}^{n_t} (m_n(\mathbf{x}_t) - f(\mathbf{x}_t))^2}}{\max_{t=1:n_t} f(\mathbf{x}_t) - \min_{t=1:n_t} f(\mathbf{x}_t)}, \quad (11)$$

wherein  $\{(\mathbf{x}_t, f(\mathbf{x}_t))\}_{t=1}^{n_t}$  is the test data set. In our experiments,  $n_t = 3000$  and the test points are spread across the domain uniformly. The total number of function evaluations is set to  $30d$  and the size of initial design is  $3d$ .

Table 1: Summary of benchmark functions

	Function name	Dimension ( $d$ )	Scale
$f_1$	Franke [18]	2	Small
$f_2$	Dette & Pepelyshev (curved) [9]	3	Small
$f_3$	Hartmann [22]	3	Small
$f_4$	Park [58]	4	Small
$f_5$	Friedman [13]	5	Medium
$f_6$	Gramacy & Lee [17]	6	Medium
$f_7$	Output transformerless (OTL) circuit [4]	6	Medium
$f_8$	Piston simulation [4]	7	Medium

To construct GPs, the R package *DiceKriging* [47] is employed. The covariance kernel is Matérn 3/2 and the unknown parameters are estimated by maximum likelihood. The Matérn covariance function is a popular choice in the computer experiments literature [5, 16]. The optimisation of the adaptive design criteria is performed via the R package *DEoptim* [43] which implements the differential evolution algorithm [56]. For each

function, the sequential sampling methods are run with ten different initial space-filling designs. Thus, we have ten sets of NRMSE for each sampling strategy. The LHS design is also repeated ten times and is obtained for all sample sizes  $3d, 4d, \dots, 30d$  using the `maximinESE_LHS` function implemented in the R package *DiceDesign* [10]. This function employs a stochastic optimisation technique to produce an LHS design based on the maximin criterion.

## 4.2 Results and discussion

The results of our numerical experiments are illustrated in Figures 3 (small-scale) and 4 (medium-scale). The algorithm VIGF (black) and PVIGF (dashed cyan) in which  $q = 4$  are compared with methods based on EIGF (red), ES-LOO (orange), MSE (blue), MICE (green), and the one-shot LHS (magenta). Each curve represents the median of ten NRMSEs. Our method outperforms the other approaches in emulating the functions  $f_2, f_4, f_5, f_6$ , and  $f_8$ , and its performance is comparable in the remaining cases ( $f_1, f_3$ , and  $f_7$ ). PVIGF has a similar performance to VIGF. While the EIGF criterion has the best performance on  $f_5$  and  $f_7$ , its results on the multimodal functions  $f_1, f_3$ , and  $f_6$  are not favourable. As explained before, it is highly likely that EIGF gets stuck in an optimum. The method based on ES-LOO is never the winning algorithm, however, its accuracy results are promising except for  $f_4$ . The MSE criterion has a good capability to predict small-scale problems where it tends to fill the space in a uniform manner. This is not the case for medium-scale functions though; MSE tends to take more samples on the boundaries in the medium (and possibly high) dimensional problems. The MICE algorithm performs poorly in all the cases due to its implementation on a discrete representation. Generally, the performance of the LHS design is comparable to the adaptive sampling approaches although it performs poorly on the physical models. The main disadvantage of the one-shot LHS design is that it can waste computational resources due to under/oversampling.

The sampling behaviour of the above methods is further explained using the *discrepancy* criterion [12, 11]. It assesses the uniformity of a design by measuring how the empirical distribution of the points in the design deviates from the uniform distribution. The  $\mathbb{L}^2$ -discrepancy of the set  $\mathbf{X}_N \subset [0, 1]^d$ , which consists of  $N$  points, is given by

$$D_2(\mathbf{X}_N) = \left[ \int_{[0,1]^d} \left| \frac{A(\mathbf{X}_N, J_{\mathbf{x}})}{N} - \text{Volume}(J_{\mathbf{x}}) \right|^2 d\mathbf{x} \right]^{1/2}. \quad (12)$$

Here,  $J_{\mathbf{x}}$  denotes the interval  $[0, \mathbf{x}) = [0, x_1) \times [0, x_2) \times \dots \times [0, x_d)$ , and  $A(\mathbf{X}_N, J_{\mathbf{x}})$  returns the number of points of  $\mathbf{X}_N$  falling in  $J_{\mathbf{x}}$  [33]. Figures 5 (small-scale) and 6 (medium-scale) show the discrepancy results of the sampling methods used in this study. As expected, the discrepancy of the LHS design is close to zero with a small variance. VIGF has neither the lowest nor highest discrepancy among the adaptive sampling approaches. This can be explain according to the characteristic of VIGF that tends to fill the space with a focus on

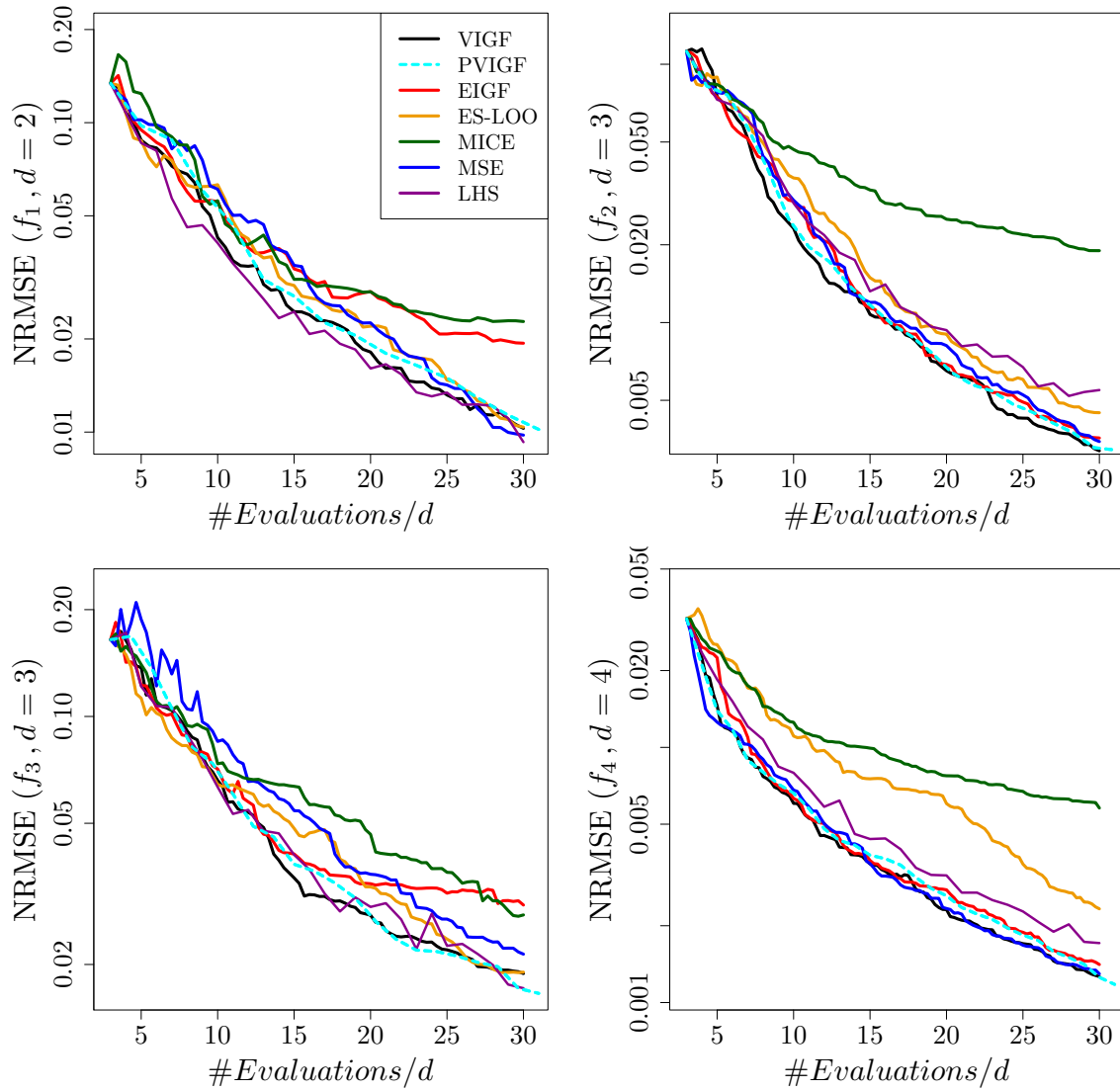


Figure 3: Accuracy results for the small-scale problems ( $1 \leq d \leq 4$ ). Each curve represents the median of ten NRMSEs for the VIGF (black), PVIGF (dashed cyan), EIGF (red), ES-LOO (orange), MSE (blue), MICE (green), and LHS (magenta) design. The latter is obtained for all sample sizes  $3d, 4d, \dots, 30d$ . The  $x$ -axis shows the number of function calls divided by the problem dimensionality. The  $y$ -axis is on a logarithmic scale.

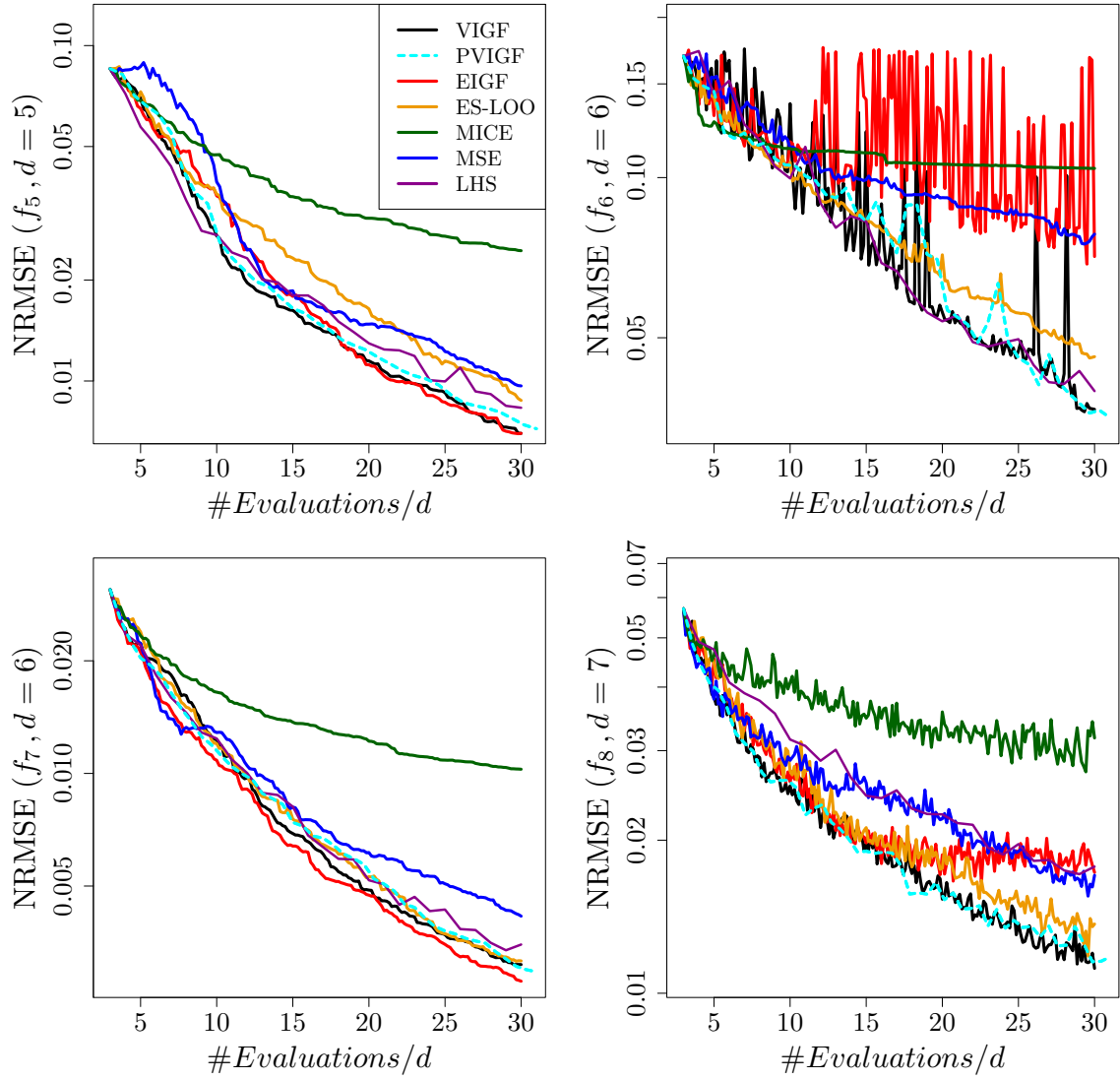


Figure 4: Accuracy results for the medium-scale problems ( $5 \leq d \leq 8$ ). Each curve is the median of ten RMSEs associated with the VIGF (black), PVIGF (dashed cyan), EIGF (red), ES-LOO (orange), MSE (blue), MICE (green), and LHS (magenta) design.

interesting regions. The discrepancy of PVIGF is close to that of VIGF. EIGF has a large discrepancy in the problems  $f_1$ ,  $f_3$ , and  $f_6$  where its performance is poor. This is due to the tendency of EIGF towards local exploitation in those problems. The designs produced by the MICE algorithm have the smallest discrepancy after the LHS method. The discrepancy of MSE is significantly larger in the medium-scale functions than small-scale ones. This indicates that many points are sampled on the boundaries of the medium-scale problems.

## 5 Conclusions

This paper presents a simple, yet effective GP-based adaptive sampling algorithm for predicting the output of complex computer codes. The method relies on the VIGF criterion to select new samples. VIGF is the variance of an improvement function defined at any location as the square of the difference between the fitted GP model and the response at the nearest site in the current design. The proposed selection criterion benefits from an efficient trade off between exploration and exploitation. As a result, the generated samples tend to fill the domain with a focus on interesting regions. We suggested the batch mode sampling via multiplying VIGF by the repulsion function relying on the GP correlation function. The performance of our method is evaluated on eight commonly used benchmark functions and the accuracy results are compared with several other sampling approaches. We observed that our method generally outperforms the other algorithms in emulating the test functions.

## Acknowledgments

The authors gratefully acknowledge the financial support of the Alan Turing Institute.

## Appendix A Test function expressions

The analytic expressions of eight test functions used in our experiments are given below.

1.  $f_1(\mathbf{x}) = 0.75 \exp\left(-\frac{(9x_1-2)^2}{4} - \frac{(9x_2-2)^2}{4}\right) + 0.75 \exp\left(-\frac{(9x_1+1)^2}{49} - \frac{9x_2+1}{10}\right) + 0.5 \exp\left(-\frac{(9x_1-7)^2}{4} - \frac{(9x_2-3)^2}{4}\right) - 0.2 \exp(-(9x_1-4)^2 - (9x_2-7)^2)$ .
2.  $f_2(\mathbf{x}) = 4(x_1 - 2 + 8x_2 - 8x_2^2)^2 + (3 - 4x_2)^2 + 16\sqrt{x_3 + 1}(2x_3 - 1)^2$ .
3.  $f_3(\mathbf{x}) = -\sum_{i=1}^4 \alpha_i \exp\left(\sum_{j=1}^3 \mathbf{A}_{ij}(x_j - \mathbf{P}_{ij})^2\right)$  where  $\alpha = (1, 1.2, 3, 3.2)^\top$ ,

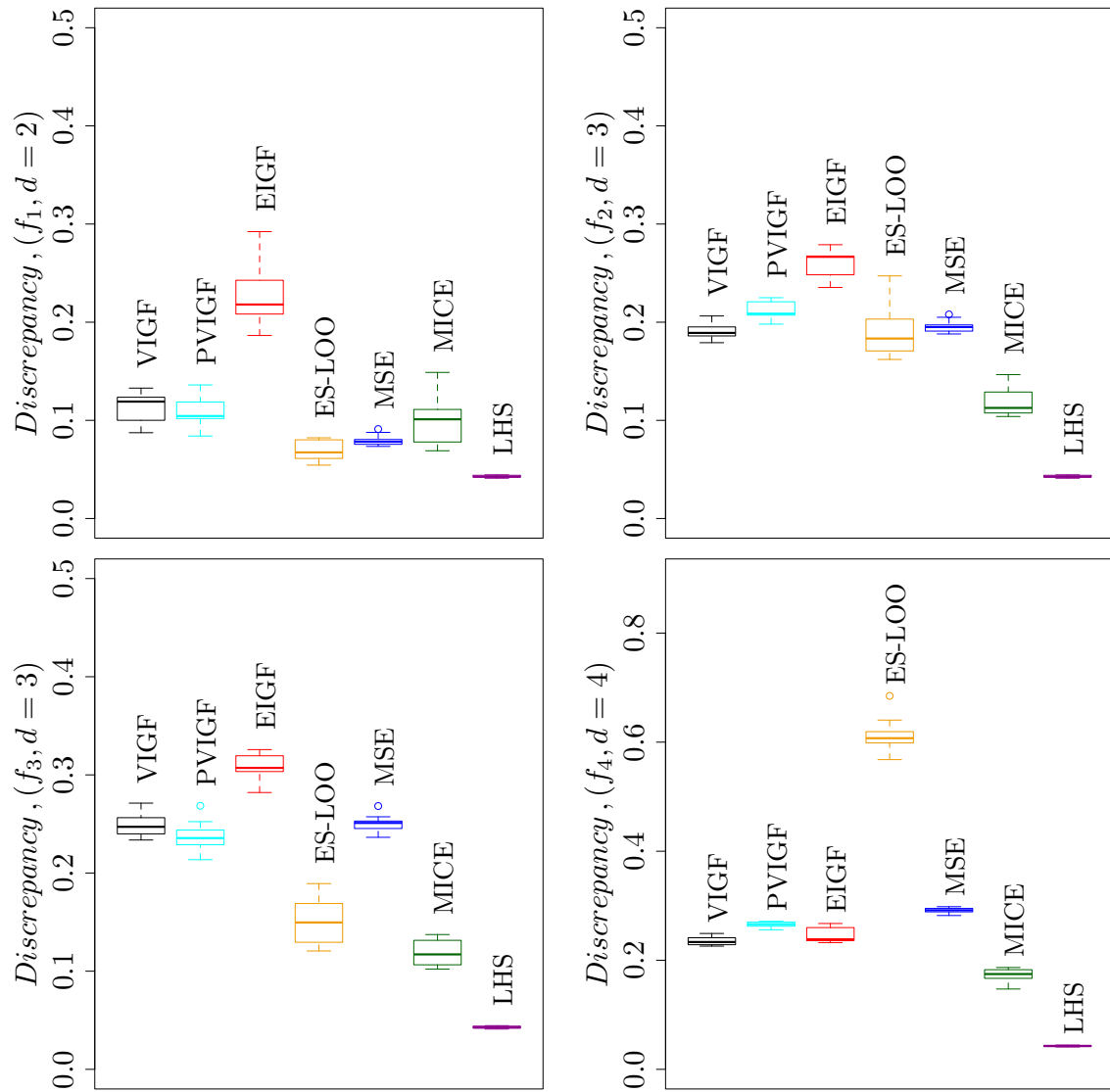


Figure 5: The box plot of the discrepancy criterion for the VIGF (black), PVIGF (cyan), EIGF (red), ES-LOO (orange), MSE (blue), MICE (green), and LHS (magenta) design. The discrepancy measures how a given distribution of points differs from the uniform distribution.

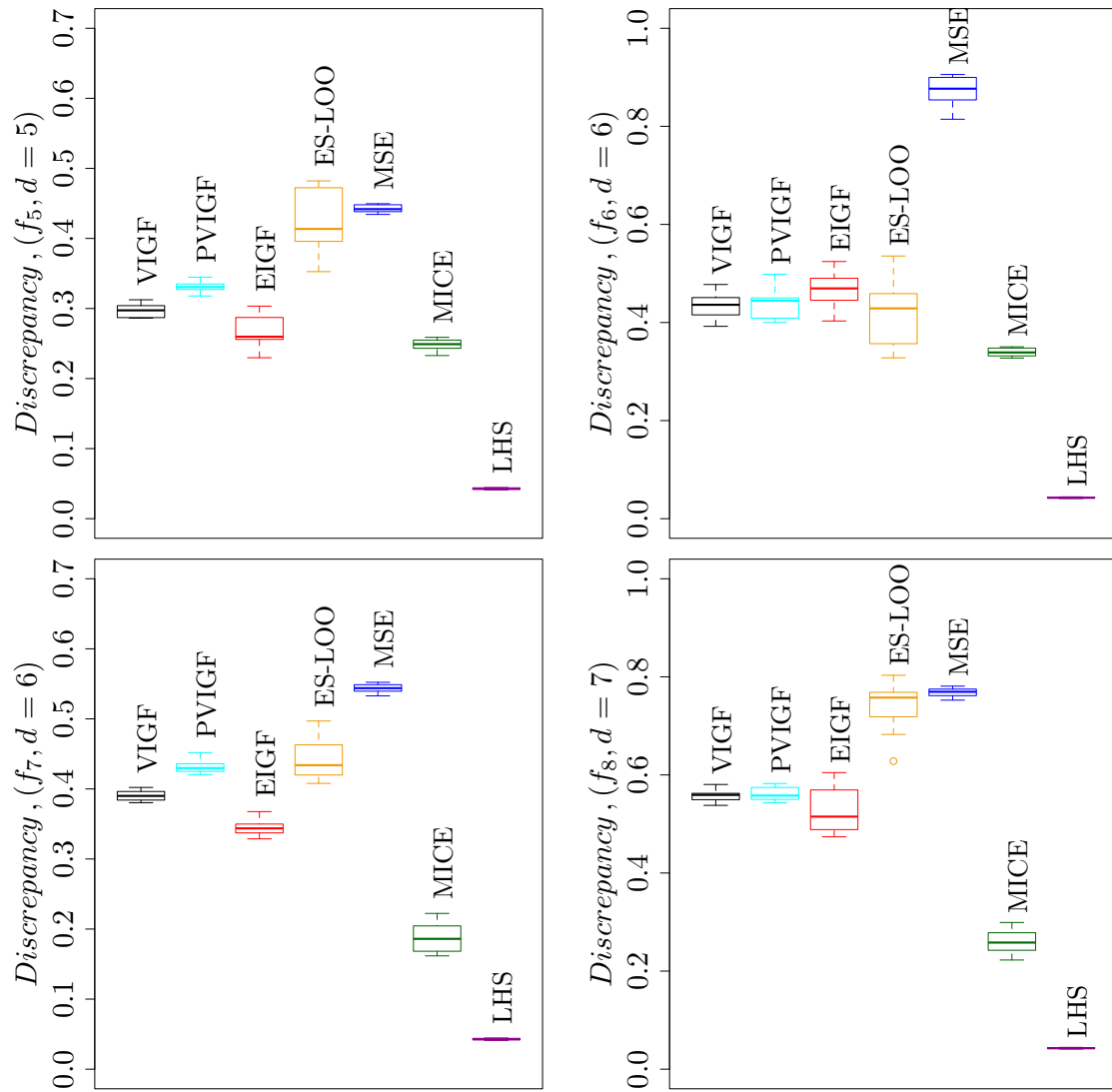


Figure 6: The box plot of the discrepancy criterion for the VIGF (black), PVIGF (cyan), EIGF (red), ES-LOO (orange), MSE (blue), MICE (green), and LHS (magenta) design.

$$\mathbf{A} = \begin{bmatrix} 3 & 10 & 30 \\ 0.1 & 10 & 35 \\ 3 & 10 & 30 \\ 0.1 & 10 & 35 \end{bmatrix}, \quad \mathbf{P} = 10^{-4} \begin{bmatrix} 3689 & 1170 & 2673 \\ 4699 & 4387 & 7470 \\ 1091 & 8732 & 5547 \\ 381 & 5743 & 8828 \end{bmatrix}.$$

4.  $f_4(\mathbf{x}) = \frac{x_1}{2} \left( \sqrt{1 + (x_2 + x_3^2) \frac{x_4}{x_1^2}} - 1 \right) + (x_1 + 3x_4) \exp(1 + \sin(x_3))$
5.  $f_5(\mathbf{x}) = 10 \sin(\pi x_1 x_2) + 20(x_3 - 0.5)^2 + 10x_4 + 5x_5.$
6.  $f_6(\mathbf{x}) = \exp(\sin([0.9(x_1 + 0.48)])^{10}) + x_2 x_3 + x_4.$
7.  $f_7(\mathbf{x}) = \frac{(V_b + 0.74)x_6(x_5 + 9)}{x_6(x_5 + 9) + x_3} + \frac{11.35x_3}{x_6(x_5 + 9) + x_3} + \frac{0.74x_3x_6(x_5 + 9)}{(x_6(x_5 + 9) + x_3)x_4}$  where  $V_b = \frac{12x_2}{x_1 + x_2}$  with:
  - $x_1 \in [50, 150]$  is the resistance  $b_1$  (K-Ohms)
  - $x_2 \in [25, 70]$  is the resistance  $b_2$  (K-Ohm)
  - $x_3 \in [0.5, 3]$  is the resistance  $f$  (K-Ohms)
  - $x_4 \in [1.2, 2.5]$  is the resistance  $c_1$  (K-Ohms)
  - $x_5 \in [0.25, 1.2]$  is the resistance  $c_2$  (K-Ohms)
  - $x_6 \in [50, 300]$  is the current gain  $c_1$  (amperes)
8.  $f_8(\mathbf{x}) = 2\pi \sqrt{\frac{x_1}{x_4 + x_2^2 \frac{x_5 x_3 x_6}{x_7 V^2}}}$  where  $V = \frac{x_2}{2x_4} \left( \sqrt{A^2 + 4x_4 \frac{x_5 x_3}{x_7} x_6} - A \right)$  and  $A = x_5 x_2 + 19.62x_1 - \frac{x_4 x_3}{x_2}$  with:
  - $x_1 \in [30, 60]$  is the piston weight (kg)
  - $x_2 \in [0.005, 0.020]$  is the piston surface area ( $m^2$ )
  - $x_3 \in [0.002, 0.010]$  is the initial gas volume ( $m^3$ )
  - $x_4 \in [1000, 5000]$  is the spring coefficient ( $N/m$ )
  - $x_5 \in [90000, 110000]$  is the atmospheric pressure ( $N/m^2$ )
  - $x_6 \in [290, 296]$  is the ambient temperature (K)
  - $x_7 \in [340, 360]$  is the filling gas temperature (K)

## References

- [1] Reza Alizadeh, Janet K. Allen, and Farrokh Mistree. Managing computational complexity using surrogate models: a critical review. *Research in Engineering Design*, 31(3):275–298, 2020.



- [2] V. Aute, K. Saleh, O. Abdelaziz, S. Azarm, and R. Radermacher. Cross-validation based single response adaptive design of experiments for kriging metamodeling of deterministic computer simulations. *Structural and Multidisciplinary Optimization*, 48(3):581–605, 2013.
- [3] J. Beck and S. Guillas. Sequential design with mutual information for computer experiments (MICE): emulation of a tsunami model. *SIAM/ASA Journal on Uncertainty Quantification*, 4(1):739–766, 2016.
- [4] Einat Neumann Ben-Ari and David M. Steinberg. Modeling data from computer experiments: An empirical comparison of kriging with mars and projection pursuit regression. *Quality Engineering*, 19(4):327–338, 2007.
- [5] Mickaël Binois, Jiangeng Huang, Robert B. Gramacy, and Mike Ludkovski. Replication or exploration? sequential design for stochastic simulation experiments. *Technometrics*, 61(1):7–23, 2019.
- [6] G. E. P. Box and J. S. Hunter. The  $2^{k-p}$  fractional factorial designs part ii. *Technometrics*, 3(4):449–458, 1961.
- [7] Kathryn Chaloner and Isabella Verdinelli. Bayesian experimental design: A review. *Statistical Science*, 10(3):273–304, 1995.
- [8] D. Austin Cole, Robert B. Gramacy, James E. Warner, Geoffrey F. Bomarito, Patrick E. Leser, and William P. Leser. Entropy-based adaptive design for contour finding and estimating reliability. *Journal of Quality Technology*, pages 1–18, 2022.
- [9] Holger Dette and Andrey Pepelyshev. Generalized Latin hypercube design for computer experiments. *Technometrics*, 52(4):421–429, 2010.
- [10] Delphine Dupuy, Céline Helbert, and Jessica Franco. DiceDesign and DiceEval: two R packages for design and analysis of computer experiments. *Journal of Statistical Software*, 65(11):1–38, 2015.
- [11] Kai-Tai Fang and Rahul Mukerjee. A connection between uniformity and aberration in regular fractions of two-level factorials. *Biometrika*, 87(1):193–198, 2000.
- [12] Kai-Tai Fang, Yuan Wang, and Peter M. Bentler. Some applications of number-theoretic methods in statistics. *Statistical Science*, 9(3):416 – 428, 1994.
- [13] Jerome H. Friedman. Multivariate adaptive regression splines. *The Annals of Statistics*, 19(1):1–67, 1991.
- [14] Jan N. Fuhg, Amélie Fau, and Udo Nackenhorst. State-of-the-art and comparative review of adaptive sampling methods for kriging. *Archives of Computational Methods in Engineering*, 28(4):2689–2747, 2021.

- [15] Sushant S. Garud, Iftekhar A. Karimi, and Markus Kraft. Design of computer experiments: a review. *Computers & Chemical Engineering*, 106:71 – 95, 2017. ESCAPE-26.
- [16] Robert B. Gramacy. *Surrogates: Gaussian Process Modeling, Design and Optimization for the Applied Sciences*. Chapman Hall/CRC, Boca Raton, Florida, 2020. <http://bobby.gramacy.com/surrogates/>.
- [17] Robert B. Gramacy and Herbert K. H. Lee. Adaptive design and analysis of super-computer experiments. *Technometrics*, 51(2):130–145, 2009.
- [18] Ben Haaland and Peter Z. G. Qian. Accurate emulators for large-scale computer experiments. *The Annals of Statistics*, 39(6):2974–3002, 2011.
- [19] J. H. Halton. On the efficiency of certain quasi-random sequences of points in evaluating multi-dimensional integrals. *Numerische Mathematik*, 2(1):84–90, 1960.
- [20] Philipp Hennig and Christian J. Schuler. Entropy search for information-efficient global optimization. *Journal of Machine Learning Research*, 13:1809–1837, 2012.
- [21] José Miguel Henrández-Lobato, Matthew W. Hoffman, and Zoubin Ghahramani. Predictive entropy search for efficient global optimization of black-box functions. In *Proceedings of the 27th International Conference on Neural Information Processing Systems*, NIPS’14, pages 918–926. MIT Press, 2014.
- [22] Momin Jamil and Xin-She Yang. A literature survey of benchmark functions for global optimization problems. *International Journal of Mathematical Modelling and Numerical Optimisation*, 4(2):150–194, 2013.
- [23] Ping Jiang, Leshi Shu, Qi Zhou, Hui Zhou, Xinyu Shao, and Junnan Xu. A novel sequential exploration-exploitation sampling strategy for global metamodeling. *IFAC-PapersOnLine*, 48(28):532–537, 2015.
- [24] Ruichen Jin, Wei Chen, and Agus Sudjianto. On sequential sampling for global metamodeling in engineering design. In *Design Engineering Technical Conferences And Computers and Information in Engineering*, volume 2, pages 539–548, 2002.
- [25] M.E. Johnson, L.M. Moore, and D. Ylvisaker. Minimax and maximin distance designs. *Journal of Statistical Planning and Inference*, 26(2):131 – 148, 1990.
- [26] Donald R. Jones. A taxonomy of global optimization methods based on response surfaces. *Journal of Global Optimization*, 21(4):345–383, Dec 2001.
- [27] Crombecq Karel, Dirk Gorissen, Dirk Deschrijver, and Tom Dhaene. A novel hybrid sequential design strategy for global surrogate modeling of computer experiments. *SIAM Journal on Scientific Computing*, 33(4):1948–1974, 2011.

- [28] Elizabeth J. Kendon, Nigel M. Roberts, Hayley J. Fowler, Malcolm J. Roberts, Steven C. Chan, and Catherine A. Senior. Heavier summer downpours with climate change revealed by weather forecast resolution model. *Nature Climate Change*, 4(7):570–576, 2014.
- [29] Mohammed Reza Kianifar and Felician Campean. Performance evaluation of meta-modelling methods for engineering problems: towards a practitioner guide. *Structural and Multidisciplinary Optimization*, 61(1):159–186, 2020.
- [30] Andreas Krause, Ajit Singh, and Carlos Guestrin. Near-optimal sensor placements in Gaussian processes: Theory, efficient algorithms and empirical studies. *Journal of Machine Learning Research*, 9:235–284, February 2008.
- [31] Chen Quin Lam. *Sequential adaptive designs in computer experiments for response surface model fit*. PhD thesis, Columbus, OH, USA, 2008. AAI3321369.
- [32] Genzi Li, Vikrant Aute, and Shapour Azarm. An accumulative error based adaptive design of experiments for offline metamodeling. *Structural and Multidisciplinary Optimization*, 40(1):137–157, 2009.
- [33] C. Devon Lin and Boxin Tang. *Handbook of Design and Analysis of Experiments*, chapter Latin hypercubes and space-filling designs. Chapman & Hall/CRC, London, 2015.
- [34] Haitao Liu, Yew-Soon Ong, and Jianfei Cai. A survey of adaptive sampling for global metamodeling in support of simulation-based complex engineering design. *Structural and Multidisciplinary Optimization*, 57(1):393–416, 2018.
- [35] Haitao Liu, Shengli Xu, Ying Ma, Xudong Chen, and Xiaofang Wang. An adaptive Bayesian sequential sampling approach for global metamodeling. *Journal of Mechanical Design*, 138(1), 2015.
- [36] A. Lopez-Perez, R. Sebastian, M. Izquierdo, R. Ruiz, M. Bishop, and J. M. Ferrero. Personalized cardiac computational models: from clinical data to simulation of infarct-related ventricular tachycardia. *Frontiers in Physiology*, 10, 2019.
- [37] Dan Maljovec, Bei Wang, Ana Kupresanin, Gardar Johannesson, Valerio Pascucci, and Peer-Timo Bremer. Adaptive sampling with topological scores. *International Journal for Uncertainty Quantification*, 3:119–141, 01 2013.
- [38] Sébastien Marmin, David Ginsbourger, Jean Baccou, and Jacques Liandrat. Warped Gaussian processes and derivative-based sequential designs for functions with heterogeneous variations. *SIAM/ASA Journal on Uncertainty Quantification*, 6(3):991–1018, 2018.

- [39] Alexandre Marques, Remi Lam, and Karen Willcox. Contour location via entropy reduction leveraging multiple information sources. In *Advances in Neural Information Processing Systems*, volume 31, page 5222–5232. Curran Associates, Inc., 2018.
- [40] M. D. McKay, R. J. Beckman, and W. J. Conover. A comparison of three methods for selecting values of input variables in the analysis of output from a computer code. *Technometrics*, 21(2):239–245, 1979.
- [41] Hossein Mohammadi, Peter Challenor, Daniel Williamson, and Marc Goodfellow. Cross-validation-based adaptive sampling for Gaussian process models. *SIAM/ASA Journal on Uncertainty Quantification*, 10(1):294–316, 2022.
- [42] Mohammad A. Mohammadi and Ali Jafarian. CFD simulation to investigate hydrodynamics of oscillating flow in a beta-type Stirling engine. *Energy*, 153:287–300, 2018.
- [43] Katharine M. Mullen, David Ardia, David L. Gil, Donald Windover, and James Cline. DEoptim: an R package for global optimization by differential evolution. *Journal of Statistical Software, Articles*, 40(6):1–26, 2011.
- [44] Art B. Owen. Orthogonal arrays for computer experiments, integration and visualization. *Statistica Sinica*, 2(2):439–452, 1992.
- [45] V. Picheny, D. Ginsbourger, O. Roustant, R. T. Haftka, and N. H. Kim. Adaptive designs of experiments for accurate approximation of a target region. *Journal of Mechanical Design*, 132(7):1–9, 2010.
- [46] Carl Edward Rasmussen and Christopher K. I. Williams. *Gaussian processes for machine learning (adaptive computation and machine learning)*. The MIT Press, 2005.
- [47] Olivier Roustant, David Ginsbourger, and Yves Deville. DiceKriging, DiceOptim: two R packages for the analysis of computer experiments by kriging-based metamodeling and optimization. *Journal of Statistical Software*, 51(1):1–55, 2012.
- [48] Jerome Sacks, William J. Welch, Toby J. Mitchell, and Henry P. Wynn. Design and analysis of computer experiments. *Statistical Science*, 4(4):409–423, 1989.
- [49] Andrea Saltelli, Stefano Tarantola, Francesca Campolongo, and Marco Ratto. *Sensitivity analysis in practice: A guide to assessing scientific models*. Wiley, 2004.
- [50] T. J. Santner, Williams B., and Notz W. *The Design and Analysis of Computer Experiments, Second Edition*. Springer-Verlag, 2018.
- [51] B. Shahriari, K. Swersky, Z. Wang, R. P. Adams, and N. de Freitas. Taking the human out of the loop: a review of Bayesian optimization. *Proceedings of the IEEE*, 104(1):148–175, 2016.

- [52] Claude Elwood Shannon. A mathematical theory of communication. *The Bell System Technical Journal*, 27(3):379–423, 1948.
- [53] Razi Sheikholeslami and Saman Razavi. Progressive Latin hypercube sampling: an efficient approach for robust sampling-based analysis of environmental models. *Environmental Modelling & Software*, 93:109 – 126, 2017.
- [54] M. C. Shewry and H. P. Wynn. Maximum entropy sampling. *Journal of Applied Statistics*, 14(2):165–170, 1987.
- [55] I.M Sobol’. On the distribution of points in a cube and the approximate evaluation of integrals. *USSR Computational Mathematics and Mathematical Physics*, 7(4):86–112, 1967.
- [56] Rainer Storn and Kenneth Price. Differential evolution – a simple and efficient heuristic for global optimization over continuous spaces. *Journal of Global Optimization*, 11(4):341–359, 1997.
- [57] Georges Voronoi. Nouvelles applications des paramètres continus à la théorie des formes quadratiques. premier mémoire. sur quelques propriétés des formes quadratiques positives parfaites. *Journal für die reine und angewandte Mathematik*, 133:97–178, 1908.
- [58] Shifeng Xiong, Peter Z. G. Qian, and C. F. Jeff Wu. Sequential design and analysis of high-accuracy and low-accuracy computer codes. *Technometrics*, 55(1):37–46, 2013.
- [59] Shengli Xu, Haitao Liu, Xiaofang Wang, and Xiaomo Jiang. A robust error-pursuing sequential sampling approach for global metamodeling based on Voronoi diagram and cross validation. *Journal of Mechanical Design*, 136(7), 04 2014.
- [60] Dawei Zhan, Jiachang Qian, and Yuansheng Cheng. Pseudo expected improvement criterion for parallel EGO algorithm. *Journal of Global Optimization*, 68(3):641–662, 2017.